Human Molecular Genetics, 2010, Vol. 19, No. 16 **3159–3168**
doi:10.1093/hmg/ddq226
Advance Access published on June 4, 2010

PTEN depletion rescues axonal growth defect and improves survival in SMN-deficient motor neurons

Ke Ning[1,†], Carsten Drepper[2,†], Chiara F. Valori[1], Mansoor Ahsan[1], Matthew Wyles[1], Adrian Higginbottom[1], Thomas Herrmann[2], Pamela Shaw[1], Mimoun Azzouz[1,*,‡] and Michael Sendtner[2,‡]

[1]Academic Neurology Unit, Department of Neuroscience, School of Medicine and Biomedical Sciences, University of Sheffield, Sheffield S10 2RX, UK and [2]Institute for Clinical Neurobiology, University of Wuerzburg, 97078 Wuerzburg, Germany

Received April 28, 2010; Revised and Accepted June 1, 2010

Phosphatase and tensin homolog (PTEN), a negative regulator of the mammalian target of rapamycin (mTOR) pathway, is widely involved in the regulation of protein synthesis. Here we show that the PTEN protein is enriched in cell bodies and axon terminals of purified motor neurons. We explored the role of the PTEN pathway by manipulating PTEN expression in healthy and diseased motor neurons. PTEN depletion led to an increase in growth cone size, promotion of axonal elongation and increased survival of these cells. These changes were associated with alterations of downstream signaling pathways for local protein synthesis as revealed by an increase in pAKT and p70S6. Most notably, this treatment also restores β-actin protein levels in axonal growth cones of SMN-deficient motor neurons. Furthermore, we report here that a single injection of adeno-associated virus serotype 6 (AAV6) expressing siPTEN into hind limb muscles at postnatal day 1 in SMNΔ7 mice leads to a significant PTEN depletion and robust improvement in motor neuron survival. Taken together, these data indicate that PTEN-mediated regulation of protein synthesis in motor neurons could represent a target for therapy in spinal muscular atrophy.

INTRODUCTION

Spinal muscular atrophy (SMA) is a devastating motor neuron disease and represents one of the most common genetic diseases leading to death in childhood (1). It is caused by mutations or deletion of the telomeric copy (*SMN1*) of the *survival motor neuron* (*SMN*) gene, leading to depletion of SMN protein levels (2). The disease is currently incurable and no effective disease-modifying treatments exist. Axonal and neuromuscular junction abnormalities are prominent pathophysiological alterations in SMA (3–6). It has been shown that reduction in Smn levels in zebrafish embryos causes axon-specific pathfinding defects in motor neurons (3). A similar finding of specific axonal defects was reported in Smn-deficient murine motor neurons (4). Reduced axon growth in Smn-deficient motor neurons correlates with reduced β-actin protein and mRNA levels in growth cones (4), suggesting that SMN is essential for the transport of mRNA within motor neurons and that disruption of this function leads to the axonal defects in SMA models (4). The exact molecular pathogenesis of SMA is unknown. The SMN protein plays a crucial role in snRNP assembly in every type of cell, including neurons. We hypothesize that intrinsic molecular signaling pathways may play a crucial role in axonal growth in motor neurons via regulation of protein synthesis. The tumor suppressor protein phosphatase and tensin homolog (PTEN) appears to be an important target based on its role in controlling the Ser/Thr kinase mammalian target of rapamycin (mTOR), which is a master regulator of protein synthesis and cell growth.

Recent studies demonstrate that the protein phosphatase activity of PTEN can regulate cell migration, spreading and growth (7). PTEN is widely expressed in mouse central nervous system (CNS) and preferentially in neurons (8). PTEN localizes to both the nucleus and cytoplasm of neuronal

*To whom correspondence should be addressed. Tel: +44 1142713204; Fax: +44 1142711711; Email: m.azzouz@sheffield.ac.uk
†These authors contributed equally to this work.
‡Joint Senior Authors.

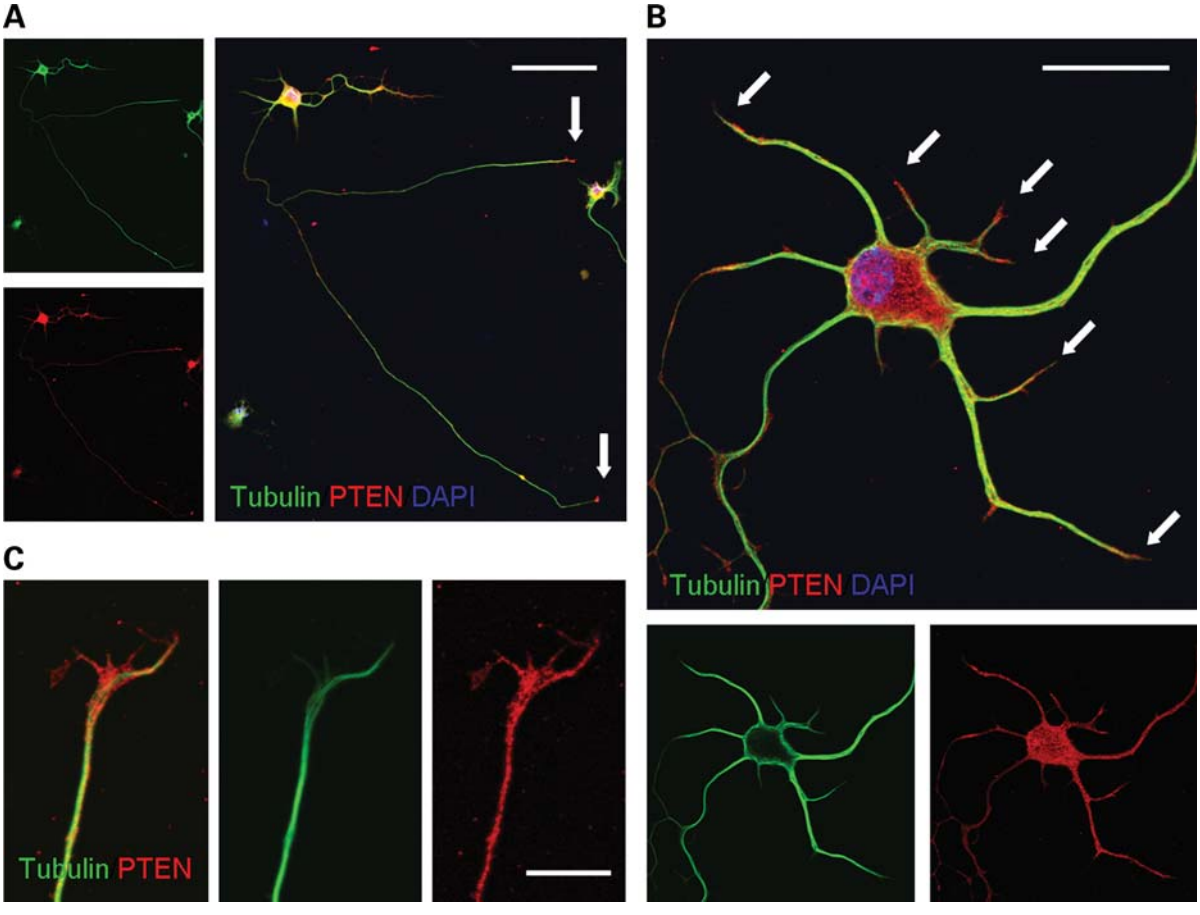

Figure 1. Localization of PTEN in cultured motor neurons. (**A**) Overview pictures of the endogenous distribution of PTEN in day 7 *in vitro* (7DIV) cultured motor neurons from wild-type mouse embryos. Prominent PTEN staining can be observed in the cell body as well as in neuritic processes. Arrows highlight PTEN immunoreactivity at active growth cones. Scale bar represents 50 μm. (**B**) Enrichment of PTEN immunoreactivity at the tips of dendrites (highlighted with arrows) in cultured motor neurons (7DIV). Scale bar represents 20 μm. (**C**) Representative image of PTEN localization at growth cones. PTEN localizes at the very fine processes of the growth cone in 7DIV cultured wild-type motor neurons. Scale bar represents 10 μm. DAPI is a nuclear counterstain (shown in blue), and the tubulin antibody stains intermediate filaments (shown in green). PTEN staining is shown in red. All images are confocal images taken with Leica SP2.

and glial cells (8–10). Significant progress has been made in exploring the broader role of PTEN in the CNS. A recent study has reported the potential of PTEN depletion to promote axonal regeneration in an experimental model of optic nerve injury (11). In addition to its normal functions such as neuronal migration (12,13) and neuronal size control (14), PTEN protein is involved in pathological processes surrounding neuronal injury such as those associated with brain ischemia, neurological and mental disorders (14–19).

Here we have generated a lentiviral vector encoding siRNA targeted against the PTEN gene and successfully used it to reduce the level of this protein in purified motor neurons. We demonstrate that PTEN depletion enhances axon growth in these cells. This treatment also restores β-actin protein levels in axonal growth cones of SMN-deficient motor neurons, indicating PTEN-mediated regulation of protein synthesis in motor neuron. Furthermore, adeno-associated virus serotype 6 (AAV6)-siPTEN delivery into hind limb muscles in SMNΔ7 mice (20), a widely used animal model of SMA, leads to robust PTEN depletion in spinal motor neurons and prevents motor neuron death.

RESULTS

Lentiviral vector-mediated efficient depletion of PTEN in motor neurons

PTEN is widely expressed in the mouse CNS. However, little is known about the expression of endogenous PTEN in spinal motor neurons. To analyze the localization pattern of the PTEN protein in motor neurons, we evaluated the protein expression using anti-PTEN antibodies in E13 primary motor neurons. We found that the PTEN protein localizes within the motor neuron cell body (Fig. 1A) but is also enriched in axonal growth cones and dendrites (Fig. 1A–C) leading us to hypothesize that PTEN may control the growth cone size and axonal elongation. We next assessed the ability of RNA interfering expression from lentivirus (LV) vectors to mediate downregulation of PTEN protein expression in wild-type spinal motor neurons. A 19 nt PTEN target sequence (19) was selected for generating an siRNA PTEN green fluorescent protein (GFP) vector that mediates the expression of PTEN siRNAs (21). A scrambled PTEN target sequence was subcloned into the lentiviral

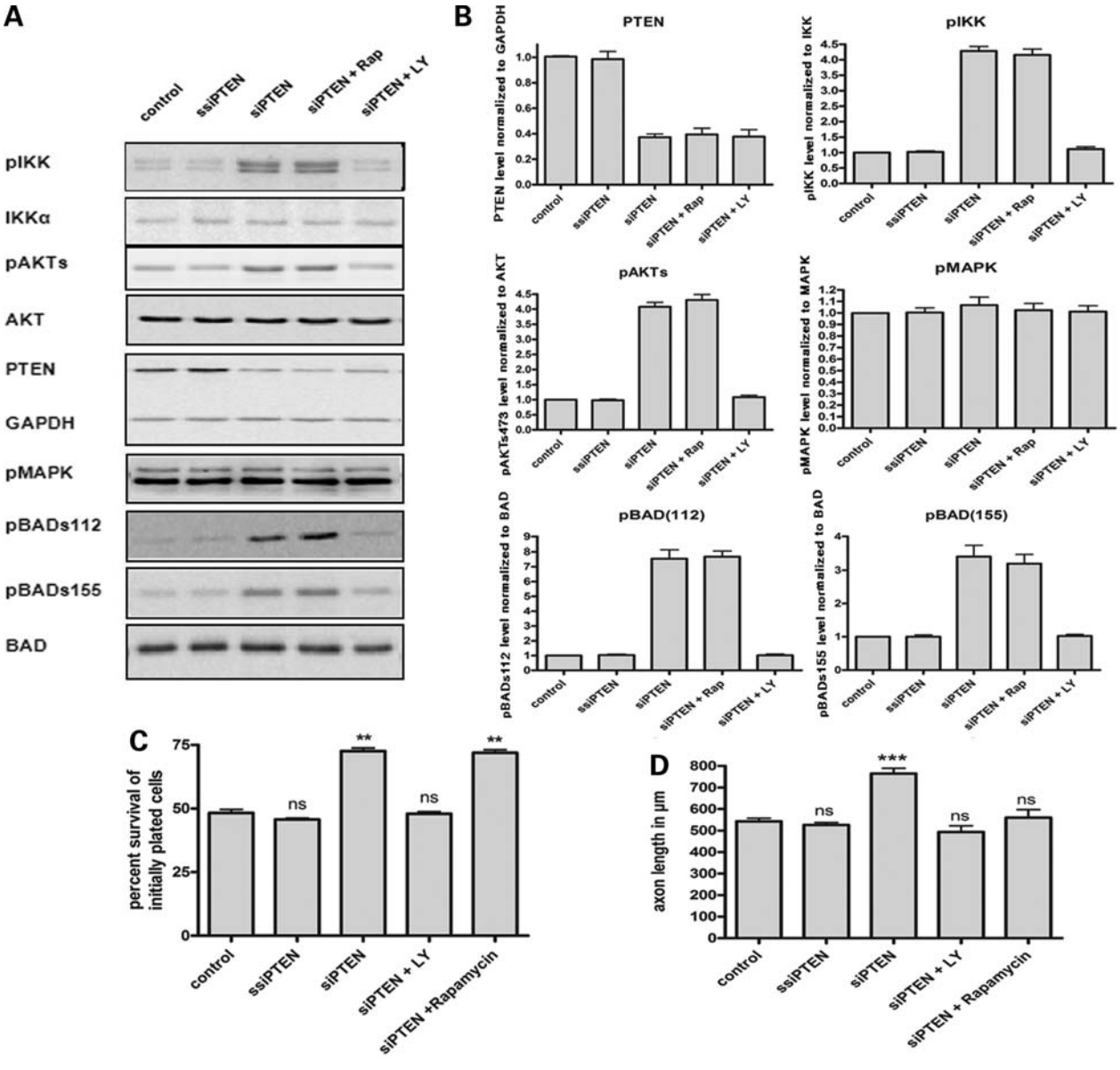

Figure 2. PTEN knock-down increases phosphorylation of IKK, AKT and BAD, but not MAPK, and influences survival and axon outgrowth. Primary motor neurons from E13 CD1 mice were cultured with or without inhibitors (LY294002 10 μM or rapamycin 10 μM). (**A**) Representative pictures of western blotting revealing that PTEN silencing in motor neurons leads to elevation of IKK, AKT and BAD phosphorylation, but no effect on MAPK was detected. (**B**) Quantification of western blot data at 7DIV. Changes in the Akt pathway were inhibited by PI3 kinase inhibitor LY294002 (10 μM), but not rapamycin 10 μM. Results represent the mean ± SEM from four independent experiments. $^{*}P < 0.05$, tested by one-way ANOVA. Cells incubated with LV-siPTEN exhibit a significant increase in survival (**C**) and axon length (**D**). Survival (percentage of originally plated cells) and average length of the longest axonal branches were scored at 7DIV. These effects of PTEN downregulation on survival and length are inhibited by PI3 kinase inhibitor, 10 μM LY294002. Note that rapamycin reverses the axonal length increase but not survival. Results represent the mean ± SEM of pooled data from four independent experiments. $^{**}P < 0.01$, $^{***}P < 0.001$, tested by one-way ANOVA.

vector and used as a control. To examine the efficacy of LV-siPTEN-mediated silencing of PTEN expression in a primary neuronal cell type, spinal motor neurons were cultured and transduced with LV-siPTEN or the control vector LV-ssiPTEN using a multiplicity of infection (MOI) of 10. High transduction efficiencies were observed, with >95% of motor neurons staining positive for GFP expression from the same viral vectors. Transduction with scrambled vector had no effect on the level of PTEN protein expression compared with untransduced controls at 6 days post-transduction (Supplementary Material, Fig. S1). Transduction with the LV-siPTEN vector, however, resulted in a significant reduction in PTEN labeling compared with LV-ssiPTEN control-transduced samples (Supplementary Material, Fig. S1). Western blot analysis of PTEN revealed 63% reduced expression at day 5 post-transduction with LV-siPTEN (Fig. 2A and B) ($P < 0.001$, one-way ANOVA with Bonferroni's post-test, $n = 4$).

PTEN depletion promotes motor neuron survival and axonal growth

We next explored whether PTEN controls motor neuron survival and axonal growth in purified motor neurons (Fig. 2C and D). Motor neurons incubated with LV-siPTEN, but not with LV-ssiPTEN control, showed significantly increased survival (Fig. 2C) ($P < 0.001$, $n = 4$ independent experiments). To assess the effects of RNAi treatment on axonal growth, motor neurons were fixed after 7 days in culture and axon length measured. Interestingly, axonal processes were significantly longer in LV-siPTEN-treated cells compared with controls (Fig. 2D) ($P < 0.001$, $n = 4$, >100 cells per condition assayed). These results indicate that PTEN depletion promotes survival and axonal growth in spinal motor neurons.

Activation of Akt by PTEN depletion promotes motor neuron survival

To objectively determine the exact intrinsic mechanisms promoting survival and axonal growth in motor neurons, we assessed potential changes in PTEN signaling pathways. It has been reported that the depletion of PTEN in cultured rat hippocampal neurons and mouse brain led to increased levels of phophorylated Akt (15,19). Consistent with these reports, our data revealed that purified motor neurons with reduced levels of PTEN show elevated Akt phosphorylation as assessed by immunostaining and western blot analysis (Supplementary Material, Fig. S1 and Fig. 2A and B). On the other hand, there is no change in MAPK phosphorylation following PTEN depletion (Fig. 2A and B). The Akt phosphorylation and enhanced motor neuron survival observed here were inhibited by the PI3K inhibitor, LY294002, but not by rapamycin (Fig. 2A–C). LV-siPTEN-mediated PTEN downregulation also results in increased phosphorylation levels of IKK and Bad in motor neurons. Together, these data reveal further evidence that modulation of PTEN can activate Akt-downstream pathways and thus exert its survival-promoting effect in motor neurons.

Activation of PTEN/mTOR pathway increase in growth cone size

Axon elongation, but not motor neuron survival, was inhibited by the mTOR inhibitor rapamycin (Fig. 2C and D) ($P < 0.001$, $n = 4$, >100 cells per condition assayed). One of the major targets of mTOR kinase is ribosomal p70S6 kinase, which in turn phosphorylates ribosomal protein S6 via S6K. We investigated this activity of the mTOR pathway, and this experiment revealed that LV-siPTEN increased the growth cone size which is correlated with an elevation in phosphorylation of p70S6K (Fig. 3C–E). LV-siPTEN also led to an increase in pS6K and pS6 levels as shown by western blot experiments (Fig. 3A and B), indicating that the increase in growth cones size observed following PTEN silencing is mediated by the activation of the PI3K/mTOR pathways which could be due to an increase in translation activity.

Pten depletion restores β-actin protein level in SMN-deficient motor neurons

We next examined the effect of PTEN depletion within diseased motor neurons, using purified motor neurons from a mouse model of SMA (4,22). This *in vitro* model has been widely used to explore disease pathophysiology in SMA (4,22,23). The depletion of PTEN led to a robust increase in axonal elongation in E13 $Smn^{-/-}$SMN2 motor neurons ($P < 0.001$, $n = 4$, >60 cells per condition assayed) (Fig. 4A). Notably, LV-siPTEN-mediated specific PTEN knock-down caused a significant increase in survival and growth cone size when compared with control motor neurons (Fig. 4B and E). Similar observations were made in motor neurons isolated from $Smn^{+/+}$ mice (Fig. 4B and E). These changes were associated with significant protein translation regulation at the growth cone as revealed by increased levels of pS6 and actin protein (Fig. 4C). The β-actin protein has been shown to be locally translated in axonal growth cones (24), and reduced axonal translocation and translation for the β-actin mRNA has been shown to be a key pathological alteration in motor neurons from Smn-deficient mouse models (4) (Fig. 4C).

PTEN downregulation allowed the restoration of β-actin protein levels in the growth cones of motor neurons (Fig. 4C) in the absence of any alteration in β-actin mRNA levels (Supplementary Material, Fig. S2). These data suggest that the beneficial effect of PTEN knock-down does not increase the amount of mRNA in the growth cone area but results from an increase in the translation which was assessed by the S6 activity (Fig. 4D). This is consistent with previous results showing that mTOR controls the translation of neuronal proteins (25,26).

PTEN depletion enhance survival of motor neurons in SMNΔ7 mice

AAV6 vectors can access spinal motor neurons via retrograde transport from axon terminals in the skeletal muscle. To explore the efficacy of PTEN gene silencing on motor neuron survival in the SMNΔ7 mouse model (20), AAV6-siPTEN or AAV6-ssiPTEN vectors were injected unilaterally into the hind limb gastrocnemius at postnatal day 1 (PN1). SMNΔ7 transgenic mice develop a severe phenotype only a few days after birth, first by a decrease in their body weight, then by motor neuron degeneration at 9 days of age. As the disease progresses, they also develop proximal muscle weakness and atrophy, resulting in end-stage paralysis and death at ~14 days of age (20). As we never established quantitatively the potential of AAV6 vectors to transduce motor neurons in mice with nerve degeneration, we first evaluated their gene transfer efficiency to motor neurons in the SMNΔ7 mouse model. The AAV6 vector genome includes the human pol III H1 promoter driving the transcription of the PTEN shRNA target sequence and the GFP reporter gene downstream from a CMV promoter.

At 10 days after injection of an AAV6 vector unilaterally in the hind limb muscles in 1-day-old SMNΔ7 mice, extensive reporter gene expression was observed in the lumbar spinal cord (Fig. 5A). When staining for calcitonin gene-related

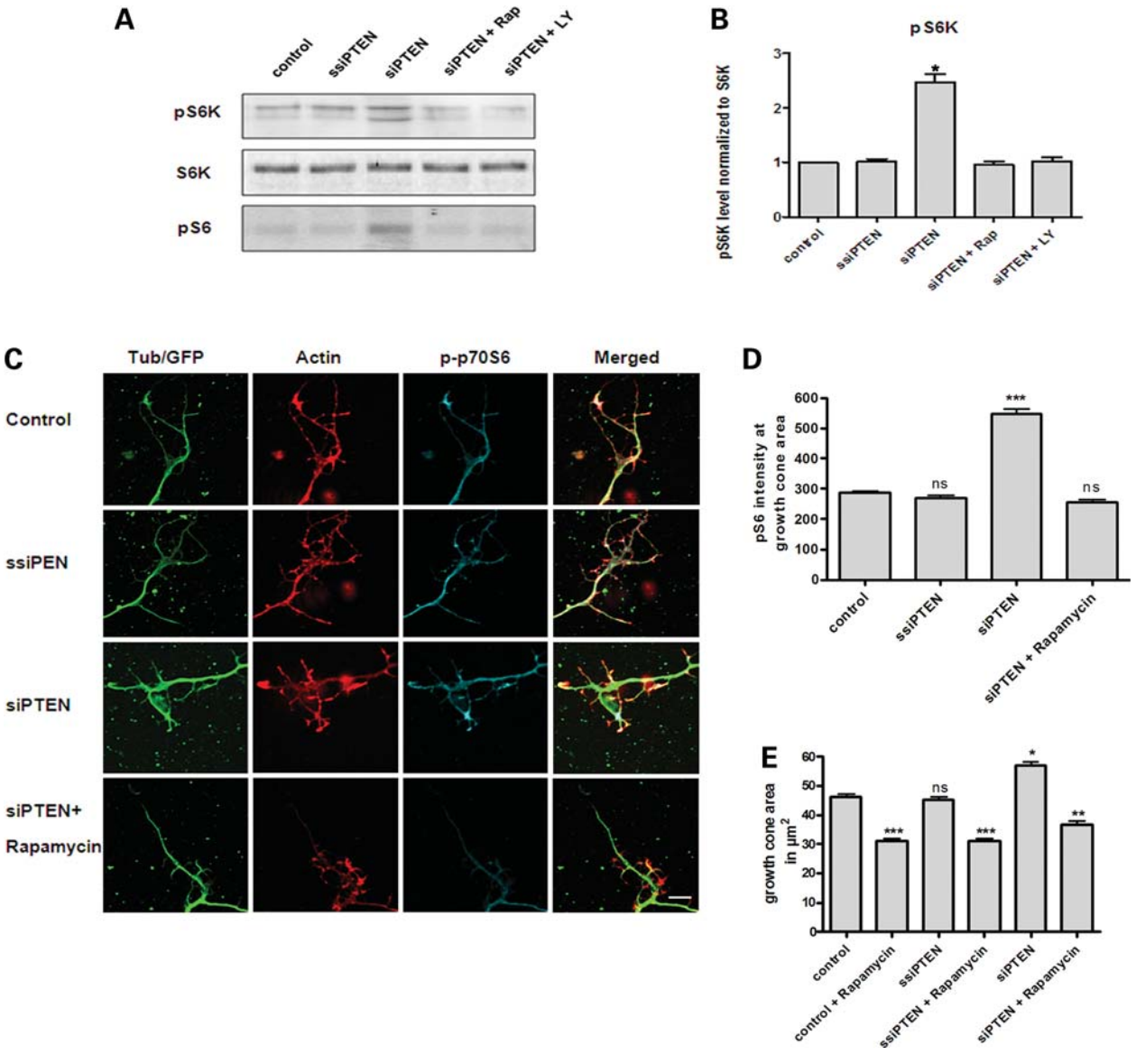

Figure 3. Role of the PTEN/mTOR pathway in controlling growth cone size in wild-type motor neurons. Primary motor neurons from CD1 mice were cultured in the presence of brain-derived neurotropic factor (BDNF). Lentiviral vectors (LV-siPTEN and LV-ssiPTEN) (MOI = 50) were added 24 h after plating. (**A**) Western blot showing elevation of phosphorylation of ribosomal S6 kinase 1 (S6K), which is a target of mTOR kinase, in CD1 motor neurons transduced with lentivirus expressing siRNA against PTEN. (**B**) Elevation in S6K phosphorylation has been reversed using PI3 kinase and mTOR inhibitors (LY294002 and rapamycin, respectively). (**C**) Motor neurons were immunostained with anti-tubulin (green processes), p70S6 antibodies (blue processes) and anti-actin (red processes). (**D**) Transduction of motor neurons with LV-siPTEN leads to an increase in the intensity of pS6 staining in the growth cone area. (**E**) PTEN silencing elevates growth cone size. These changes were abolished by the mTOR inhibitor rapamycin (D and E). Scale bar represents 5 µm. Results represent the mean ± SEM of pooled data from four independent experiments. $^{*}P<0.05$, $^{**}P<0.01$, $^{***}P<0.001$, tested by one-way ANOVA.

peptide (CGRP) to identify the motor neurons more directly, we found that ~40% of CGRP-positive motor neurons were transduced (Fig. 5C). Retrograde transduction of spinal motor neurons with AAV6-siPTEN resulted in a significant reduction in PTEN expression compared with control transduced cells as revealed by anti-PTEN staining (Fig. 5A). The effect of PTEN depletion on the number of motor neurons in the spinal cord was evaluated 10 days post-vector delivery. Histological evaluation of the lumbar spinal cord revealed that retrograde delivery of siRNA against PTEN in SMNΔ7 mice induced significant sparing of spinal motor neurons, with a notable >35% increase in motor neuron survival (Fig. 5A). Cell counts revealed that the percentage of CGRP-positive motor neurons was significantly higher in AAV6-siPTEN-treated mice than in AAV6-ssiPTEN control mice (137.3 ± 7.5 versus 101.2 ± 9.4% CGRP-positive motor neurons normalized to the uninjected side; $n = 3$; $P < 0.05$; Fig. 5B). This increase in survival appears confined to AAV6-siPTEN-transduced motor neruons, and only the subpopulation of motor neurons that stained positive for the reporter gene GFP showed increased survival (Fig. 5C). The number of untransduced motor neurons was similar in both

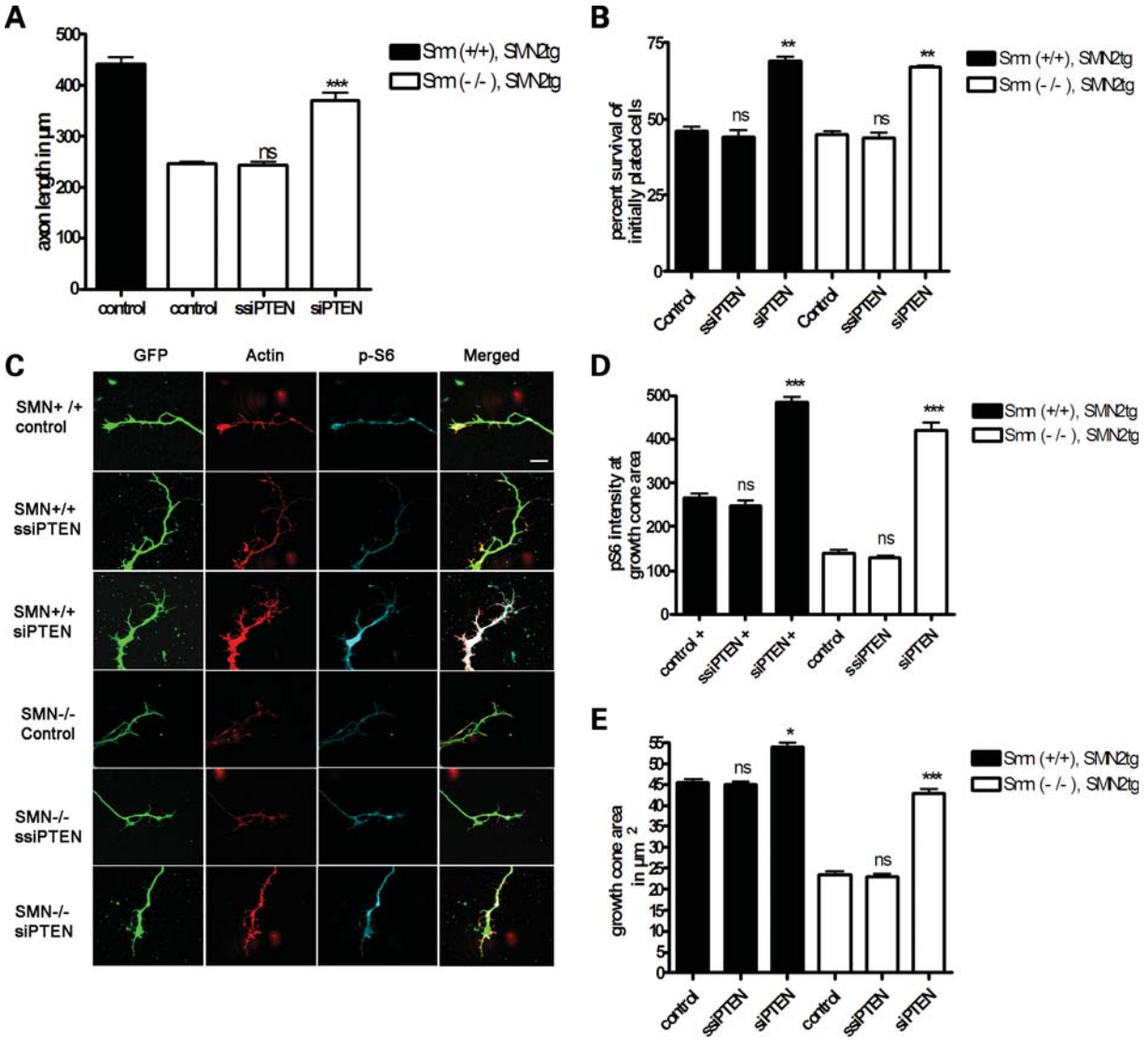

Figure 4. PTEN knock-down rescues axon length, increases survival and restores growth cone size in diseased Smn-deficient motor neurons. Primary motor neurons isolated from E13 $Smn^{-/-}$SMN2 mice were cultured in the presence of BDNF. (**A**) PTEN silencing with LV-siPTEN rescues the axon length defect in Smn-deficient motor neurons. (**B**) Cells transduced in LV-siPTEN exhibit a significant increase in survival compared with controls. (**C**) Immunostaining of fixed cells with antibodies against actin (red processes) and pS6 (blue processes). $SMN^{+/+}$ and $SMN^{-/-}$ motor neurons transduced with LV-siPTEN exhibit robust elevation of pS6 staining intensity in the growth cone area (arrows). (**D**) Quantification of pS6 staining in growth cones. (**E**) PTEN silencing restores growth cone size in $SMN^{-/-}$ motor neurons. Results represent the mean ± SEM of pooled data from four independent experiments. $^{*}P < 0.05$, $^{**}P < 0.01$, $^{***}P < 0.001$, tested by one-way ANOVA.

groups (Fig. 5D). Histological analysis showed strong GFP staining in AAV6-injected gastrocnemius muscles (Supplementary Material, Fig. S3). These data indicate the therapeutic potential of PTEN pathway modulation for the treatment of motor neuron disease.

DISCUSSION

In summary, our data indicate that the modulation of PTEN plays an important role in promoting survival and axonal growth in healthy and diseased motor neurons. Our approach achieves significant improvement in cell survival and growth cone size in Smn-deficient and healthy motor neurons, suggesting that PTEN depletion effects were not specific to diseased cells. However, it is worth highlighting that the most significant increase in growth cone size was reported in $Smn^{-/-}$ motor neurons. Our studies also reveal that activation of the mTOR pathway is sufficient to trigger protein translational regulation leading to robust axonal growth as assessed by the increase in β-actin protein level. Our data suggest that modulation of the PTEN/mTOR pathway also restores the specific pathological effects in motor neurons from a mouse model of SMA (Supplementary Material, Fig. S4).

We also report here that intramuscular delivery of AAV6 expressing siRNA against PTEN can achieve substantial improvement in motor neuron survival in the SMNΔ7 model of SMA. There is growing evidence that PTEN has an important

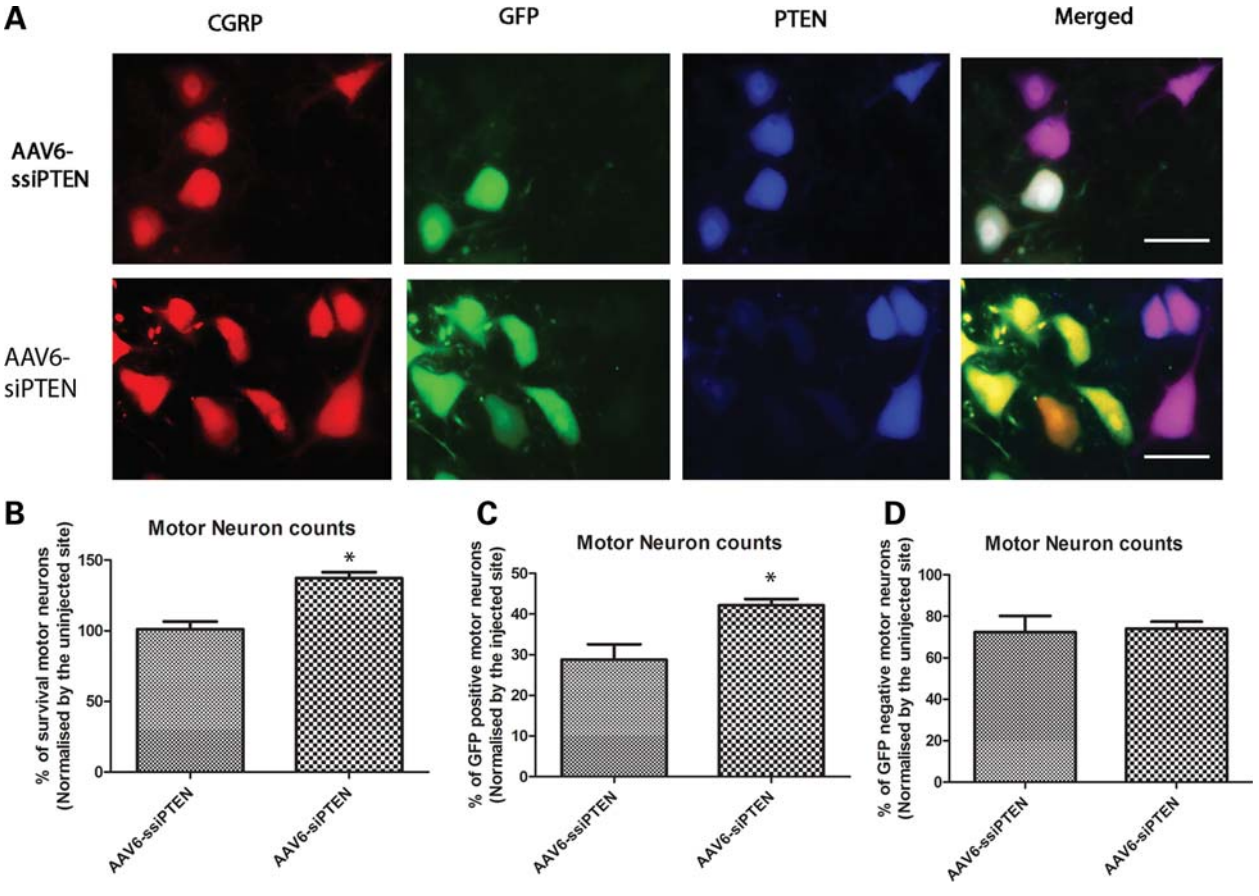

Figure 5. Motor neuron survival is enhanced by RNAi-mediated reduction in PTEN expression in SMNΔ7 transgenic mice after AAV6-siPTEN muscle gene transfer. Immunohistochemistry showing a reduction in PTEN expression in AAV6-siPTEN-transduced motor neurons (as revealed by anti-PTEN and GFP labeling) compared with AAV6-ssiPTEN controls (**A**). CGRP staining was used to identify spinal motor neurons (A). Cell counts of total surviving lumbar spinal cord motor neurons (normalized to the uninjected side) in AAV6-siPTEN- and AAV6-ssiPTEN-treated SMNΔ7 mice at 10 days of age (**B**). Quantification of total GFP-positive (**C**) and negative (**D**) motor neurons. Scale bars: 20 μm; $^{*}P < 0.05$, Student's test, $n = 3$).

role in CNS disorders (reviewed in 27). A previous study has reported the potential of PTEN depletion to promote axonal regeneration in an experimental model of optic nerve injury (11). Although PTEN and Akt have been reported to be important for neuronal survival, this is the first report to demonstrate the role of the PTEN pathway in axonal growth and motor neuron survival in a disease model. Thus, the manipulation of the PTEN/mTOR pathway may represent an important therapeutic strategy to promote the health of the distal axon and motor neuron survival in SMA and probably also other forms of motor neuron disease.

MATERIALS AND METHODS

siRNA design and viral production

A 19 nt sequence targeting mouse PTEN (19) was subcloned in the pLVTHM genome vector (28) (Addgene plasmid 12247) according to the manufacturer's protocol. Briefly, siPTEN sense oligonucleotide 5′-CGCGTCCCCGCCAAA TTTAACTGCAGAGTTCAAGAGACTCTGCAGTTAAATT TGGCTTTTTGGAAAT and siPTEN antisense oligonucleotide 5′-CGATTTCCAAAAAGCCAAATTTAACTGCAGAG TCTCTTGAACTCTGCAGTTAAATTTGGCGGGGA were annealed and cloned into the *Mlu*I/*Cla*I-digested vector. Accordingly, ssiPTEN sense nucleotide 5′-CGCGTCCCC CGCAATATTCAATCGAGGATTCAAGAGATCCTCGATT GAATATTGCGTTTTTGGAAAT and ssiPTEN antisense nucleotide 5′-CGATTTCCAAAAACGCAATATTCAATCG AGGATCTCTTGAATCCTCGATTGAATATTGCGGGGGA were used to generate the control LV-ssiPTEN vector. This approach allowed us to generate a stem–loop (21)–stem shRNA to effectively reduce PTEN expression levels.

The third generation of self-inactivating (SIN) lentiviral vector stocks involving four plasmids (pMD.2G, pCMVDR8.92, SIN-W-PGK, pRSV-Rev) were prepared by transient calcium phosphate transfection of the human embryonic kidney 293T cell line as previously described (29). These vectors were pseudotyped with the vesicular stomatitis virus-G envelope protein. Viral titers were estimated using the p24 capsid protein measured by enzyme-linked immunosorbent assay (29). AAV6 production has been performed as described in Gregorevic *et al*. (30).

Motor neuron culture

Cultures of embryonic spinal motor neurons were prepared essentially as described in Wiese *et al*. (22). Briefly, the ventrolateral part of the E13 spinal cord was dissected and incu-

bated for 15 min in 0.05% trypsin in Hanks' balanced salt solution. After trituration, cells were plated on dishes pre-coated with anti-p75 NGF receptor antibody (Abcam, ME20.4, ab8877) in Neurobasal (Gibco) for 30 min. The cells were washed three times with Neurobasal, and the attached cells were isolated from the plate with depolarizing solution (0.8% NaCl, 35 mM KCl) and collected in full media [Neurobasal supplemented with 2% horse serum, 1× B27 (Gibco) and 1× Glutamax (Gibco)]. For staining, 2000 cells were plated on poly-DL-ornithine (Sigma) and mouse laminin (Invitrogen) coated coverslips in 4-well dishes (Greiner) and processed as described below. For survival assays, 1500 cells were plated without coverslips in 4-well dishes coated with poly-ornithine and mouse laminin. Cells were observed under a phase-contrast microscope (Leica) and the number of initially plated cells was determined after the cells were attached 6 h after plating. After 7 days of culture, the number of surviving cells was counted. For western blots 200 000 cells were plated on three 5 cm cell culture dishes (Falcon) also coated with poly-ornithine and mouse laminin. For all assays, brain-derived neurotropic factor was used at concentrations of 5 ng/ml and motor neurons were cultured for 7 days at 37°C with 5% CO_2. Medium was replaced after 24 h and then every 2 days. For some experiments, inhibitors were used at 10 μM concentrations (rapamycin and LY294002, from Calbiochem).

Animals

All the procedures involving animals were performed according to the UK Home Office regulations. SMNΔ7 mice (20) were purchased from The Jackson Laboratory (stock #005025) and were maintained in a controlled facility in a 12 h dark/12 h light photocycle with free access to food and water. Carrier animals were used for breeding and the offspring were genotyped immediately after birth by PCR amplification of the transgenes according to the protocols provided by The Jackson Laboratory.

AAV6-siPTEN ($n = 3$) or AAV6-ssiPTEN ($n = 3$) vectors were injected unilaterally into the hind limb gastrocnemius and levator auris longus muscles of SMNΔ7 mice at PN1. AAV6 vectors ($\sim 10^{11}$ vector genome) were delivered under isoflurane general anesthesia. The mice were then allowed to recover, rolled in the sawdust from their original cage and immediately returned to their cage. Animals were terminally anesthetized with penthobarbital at PN10. Relevant tissues were fixed in 4% PFA for 48 h, then cryoprotected in 30% sucrose and mounted in optimal cutting temperature. Spinal cord sections of 20 μm thickness were prepared on a sliding cryostat microtome (Leica) and collected onto gelatine-coated microscope slides. Immunohistochemistry was then performed with rabbit anti-CGRP (1:3000; Sigma-Aldrich) and mouse anti- PTEN (1:200; Cell Signaling) followed by goat anti-mouse Cy3 (1:200; Jackson Laboratories) and goat anti rabbit FITC (1:200; Jackson Laboratories).

Motor neuron counts

Lumbar spinal motor neurons were identified using anti-CGRP antibodies. Serial sections of L1–L6 spinal cord were used for cell counts of total CGRP-positive cells in injected and contralateral sides of AAV6-siPTEN ($n = 3$) and AAV6-SsiPTEN ($n = 3$) mice. The percentage of total motor neurons (CGRP positive) in the treated side was normalized by the uninjected side. Transduced motor neurons were identified by the reporter marker GFP. We therefore counted the number of GFP-positive motor neurons in both AAV6-siPTEN and AAV6-SsiPTEN control. The percentage of GFP positive motor neurons was normalized by total motor neuron (CGRP-positive cells) number in the treated side. The percentage of GFP-negative motor neurons (untransduced motor neurons) on the injected site was normalized by total motor neuron number.

Immunocytochemistry

Immunocytochemistry was performed as described previously (4). The following primary antibodies were used: rabbit polyclonal antibodies against pAKT (1:200; Cell Signaling), pS6 ser235/236 (1:200; Cell Signaling), pIKK (1:200; Cell Signaling), mouse monoclonal antibodies against β-actin (1:500; Abcam), microtubule-associated protein 2 (1:500; Sigma-Aldrich) and PTEN (1:200; Cell Signaling). Cells were then washed three times with 1× TBS-T (20 mM Tris–HCl, pH 7.6, 137 mM NaCl and 0.1% Tween-20) and incubated for 1 h at room temperature with Cy2-(1:200) or Cy3-(1:300) conjugated secondary antibodies (Dianova). Confocal images were obtained with an SP2 or SP5 microscope (Leica).

Western blot analysis

Primary motor neurons were transduced with lentivirus for 5 days with or without inhibitors (10 μM LY294002 or rapamycin, both Calbiochem) and collected from the dishes. Protein extraction for western blotting was performed as described previously (4). Primary antibodies, anti-mouse GAPDH antibody (1:5000; Calbiochem), anti-rabbit PTEN (1:1000; Cell Signaling), AKT (1:1000; Cell Signaling), Bad (1:1000; Cell Signaling), MAPK (1:1000; Cell Signaling), pAKT ser473 (1:1000; Cell Signaling), p-Bad ser155 (1:1000; Cell Signaling), p-Bad ser112 (1:1000; Cell Signaling), IKKa (1:1000; Calbiochem), pIKK (1:1000; Calbiochem), S6K (1:1000; Cell Signaling), pS6K (1:1000; Cell Signaling) and pS6 (1:1000; Cell Signaling) were used.

In situ hybridization

All solutions and equipment were treated with 0.1% diethylpyrocarbonate (Sigma) and autoclaved. All washes were at room temperature unless stated otherwise. Motor neurons were cultured for 5 days *in vitro* and fixed for 15 min in 4% paraformaldehyde. Coverslips were washed three times in PBS (pH7.4) and permeabilized in 0.3% Triton X-100 in PBS for 30 min. Coverslips were then washed three times with PBS for 15 min each. Pre-hybridization was performed in hybridization buffer (Sigma) for 1 h at 37°C. Cells were hybridized overnight with 100 ng/ml GreenStar biotin oligonucleotide probe against β-actin mRNA (Gene Detect, antisense probe). Hybridization with sense probe and poly(dT)-control were also performed simultaneously. Cells were washed twice at 56°C with 1× SSC + 10 mM DTT, followed by 0.5× SSC +10 mM DTT twice and equilibrated in

tris buffered saline tween-20 (TBST). Cells were incubated with streptavidin–horseradish peroxidase (DAKO) at a dilution of 1:100 for 20 min, then washed three times with TBST for 5 min each. The signal was amplified by incubating with biotinylated-tyramide (DAKO) for 20 min at room temperature followed by washing three times with TBST. Finally, the cells were treated with avidin–rhodamine at a dilution of 1:100 for 15 min and coverslips were mounted on a slide using Mowiol. Pictures were taken with a Leica SP2 confocal microscope and quantification was performed with the LAS AF Lite Software (version 2.0.2_2038, Leica).

Data analysis

Axons of motor neurons were identified by their length as processes that are at least twice as long as dendrites. Only the longest axonal branches were measured. Cultures obtained from mutant and control embryos from different litters were analyzed after staining under a confocal microscope (SP2, Leica), and axon length was measured from pictures using imaging software (Leica Confocal Software, Leica). Background intensity was measured for every single picture and subtracted. The final processing of all images was performed with Photoshop 7.0 (Adobe). Values from at least three independent experiments were pooled and the results were expressed as the mean $\pm$ SEM. Statistical significance of differences was assessed by one-way analysis of variance and Bonferroni's post-test after using Prism software (GraphPad).

SUPPLEMENTARY MATERIAL

Supplementary Material is available at *HMG* online.

ACKNOWLEDGEMENTS

We thank Nicole Déglon for providing us with lentiviral vector plasmids and technical advice on viral production.

Conflict of Interest statement. None declared.

FUNDING

This work was supported by the SMA Trust (through SMA Europe), the Hermann und Lillly Schilling Stiftung im Stifterverband der Deutschen Industrie and by the Deutsche Forschungsgemeinschaft, SFB 581, TP B1.

REFERENCES

1. Burghes, A.H. and Beattie, C.E. (2009) Spinal muscular atrophy: why do low levels of survival motor neuron protein make motor neurons sick? *Nat. Rev. Neurosci.*, **10**, 597–609.
2. Lefebvre, S., Burglen, L., Reboullet, S., Clermont, O., Burlet, P., Viollet, L., Benichou, B., Cruaud, C., Millasseau, P. and Zeviani, M.E.A. (1995) Identification and characterization of a spinal muscular atrophy-determining gene. *Cell*, **80**, 155–165.
3. McWhorter, M.L., Monani, U.R., Burghes, A.H.M. and Beattie, C.E. (2003) Knockdown of the survival motor neuron (Smn) protein in zebrafish causes defects in motor axon outgrowth and pathfinding. *J. Cell Biol.*, **162**, 919–931.
4. Rossoll, W., Jablonka, S., Andreassi, C., Kröning, A.K., Karle, K., Monani, U.R. and Sendtner, M. (2003) Smn, the spinal muscular atrophy-determining gene product, modulates axon growth and localization of beta-actin mRNA in growth cones of motoneurons. *J. Cell Biol.*, **163**, 801–812.
5. Jablonka, S., Wiese, S. and Sendtner, M. (2004) Axonal defects in mouse models of motoneuron disease. *J. Neurobiol.*, **58**, 272–286.
6. Kong, L., Wang, X., Choe, D.W., Polley, M., Burnett, B.G., Bosch-Marce, M., Griffin, J.W., Rich, M.M. and Sumner, C.J. (2009) Impaired synaptic vesicle release and immaturity of neuromuscular junctions in spinal muscular atrophy mice. *J. Neurosci.*, **29**, 842–851.
7. Tamura, M., Gu, J., Danen, E.H., Takino, T., Miyamoto, S. and Yamada, K.M. (1999) PTEN interactions with focal adhesion kinase and suppression of the extracellular matrix-dependent phosphatidylinositol 3-kinase/Akt cell survival pathway. *J. Biol. Chem.*, **274**, 20693–20703.
8. Lachyankar, M.B., Sultana, N., Schonhoff, C.M., Mitra, P., Poluha, W., Lambert, S., Quesenberry, P.J., Litofsky, N.S., Recht, L.D., Nabi, R. *et al.* (2000) A role for nuclear PTEN in neuronal differentiation. *J. Neurosci.*, **20**, 1404–1413.
9. Sano, T., Lin, H., Chen, X., Langford, L.A., Koul, D., Bondy, M.L., Hess, K.R., Myers, J.N., Hong, Y.K., Yung, W.K. *et al.* (1999) Differential expression of MMAC/PTEN in glioblastoma multiforme: relationship to localization and prognosis. *Cancer Res.*, **59**, 1820–1824.
10. Li, L., Liu, F. and Ross, A.H. (2003) PTEN regulation of neural development and CNS stem cells. *J. Cell Biochem.*, **88**, 24–28.
11. Park, K.K., Liu, K., Hu, Y., Smith, P.D., Wang, C., Cai, B., Xu, B., Connolly, L., Kramvis, I., Sahin, M. *et al.* (2008) Promoting axon regeneration in the adult CNS by modulation of the PTEN/mTOR pathway. *Science*, **322**, 963–966.
12. Li, L., Liu, F., Salmonsen, R.A., Turner, T.K., Litofsky, N.S., Di Cristofano, A., Pandolfi, P.P., Jones, S.N., Recht, L.D. and Ross, A.H. (2002) PTEN in neural precursor cells: regulation of migration, apoptosis, and proliferation. *Mol. Cell. Neurosci.*, **20**, 21–29.
13. Leslie, N.R., Yang, X., Downes, C.P. and Weijer, C.J. (2005) The regulation of cell migration by PTEN. *Biochem. Soc. Trans.*, **33**, 1507–1508.
14. Kwon, C.H., Zhu, X., Zhang, J., Knoop, L.L., Tharp, R., Smeyne, R.J., Eberhart, C.G., Burger, P.C. and Baker, S.J. (2001) Pten regulates neuronal soma size: a mouse model of Lhermitte–Duclos disease. *Nat. Genet.*, **29**, 404–411.
15. Groszer, M., Erickson, R., Scripture-Adams, D.D., Lesche, R., Trumpp, A., Zack, J.A., Kornblum, H.I., Liu, X. and Wu, H. (2001) Negative regulation of neural stem/progenitor cell proliferation by the Pten tumor suppressor gene *in vivo*. *Science*, **294**, 2186–2189.
16. Kwon, C.H., Luikart, B.W., Powell, C.M., Zhou, J., Matheny, S.A., Zhang, W., Li, Y., Baker, S.J. and Parada, L.F. (2006) Pten regulates neuronal arborization and social interaction in mice. *Neuron*, **50**, 377–388.
17. Omori, N., Jin, G., Li, F., Zhang, W.R., Wang, S.J., Hamakawa, Y., Nagano, I., Manabe, Y., Shoji, M. and Abe, K. (2002) Enhanced phosphorylation of PTEN in rat brain after transient middle cerebral artery occlusion. *Brain Res.*, **954**, 317–322.
18. Gary, D.S. and Mattson, M.P. (2002) PTEN regulates Akt kinase activity in hippocampal neurons and increases their sensitivity to glutamate and apoptosis. *Neuromol. Med.*, **2**, 261–269.
19. Ning, K., Pei, L., Liao, M., Liu, B., Zhang, Y., Jiang, W., Mielke, J.G., Li, L., Chen, Y., El-Hayek, Y.H. *et al.* (2004) Dual neuroprotective signaling mediated by downregulating two distinct phosphatase activities of PTEN. *J. Neurosci.*, **24**, 4052–4060.
20. Le, T.T., Pham, L.T., Butchbach, M.E., Zhang, H.L., Monani, U.R., Coovert, D.D., Gavrilina, T.O., Xing, L., Bassell, G.J. and Burghes, A.H. (2005) SMNDelta7, the major product of the centromeric survival motor neuron (*SMN2*) gene, extends survival in mice with spinal muscular atrophy and associates with full-length SMN. *Hum. Mol. Genet.*, **14**, 845–857.
21. Brummelkamp, T.R., Bernards, R. and Agami, R. (2002) A system for stable expression of short interfering RNAs in mammalian cells. *Science*, **296**, 550–553.
22. Wiese, S., Pei, G., Karch, C., Troppmair, J., Holtmann, B., Rapp, U.R. and Sendtner, M. (2001) Specific function of B-Raf in mediating survival of embryonic motoneurons and sensory neurons. *Nat. Neurosci.*, **4**, 137–142.
23. Jablonka, S., Beck, M., Lechner, B.D., Mayer, C. and Sendtner, M. (2007) Defective Ca^{2+} channel clustering in axon terminals disturbs excitability in motoneurons in spinal muscular atrophy. *J. Cell Biol.*, **179**, 139–149.

24. Zhang, H.L., Eom, T., Oleynikov, Y., Shenoy, S.M., Liebelt, D.A., Dictenberg, J.B., Singer, R.H. and Bassell, G.J. (2001) Neurotrophin-induced transport of a beta-actin mRNP complex increases beta-actin levels and stimulates growth cone motility. *Neuron*, **31**, 261–275.
25. Morita, T. and Sobue, K. (2009) Specification of neuronal polarity regulated by local translation of CRMP2 and Tau via the mTOR-p70S6K pathway. *J. Biol. Chem.*, **284**, 27734–27745.
26. Endersby, R. and Baker, S.J. (2008) PTEN signaling in brain: neuropathology and tumorigenesis. *Oncogene*, **27**, 5416–5430.
27. Chang, N., El-Hayek, Y.H., Gomez, E. and Wan, Q. (2007) Phosphatase PTEN in neuronal injury and brain disorders. *Trends Neurosci.*, **30**, 581–586.
28. Wiznerowicz, M. and Trono, D. (2003) Conditional suppression of cellular genes: lentivirus vector-mediated drug-inducible RNA interference. *J. Virol.*, **77**, 8957–8961.
29. Déglon, N., Tseng, J.L., Bensadoun, J.C., Zurn, A.D., Arsenijevic, Y., Pereira de Almeida, L., Zufferey, R., Trono, D. and Aebischer, P. (2000) Self-inactivating lentiviral vectors with enhanced transgene expression as potential gene transfer system in Parkinson's disease. *Hum. Gene Ther.*, **11**, 179–190.
30. Gregorevic, P., Blankinship, M.J., Allen, J.M., Crawford, R.W., Meuse, L., Miller, D.G., Russell, D.W. and Chamberlain, J.S. (2004) Systemic delivery of genes to striated muscles using adeno-associated viral vectors. *Nat. Med.*, **10**, 828–834.